ELECTRONIC OFFPRINT

Use of this pdf is subject to the terms described below

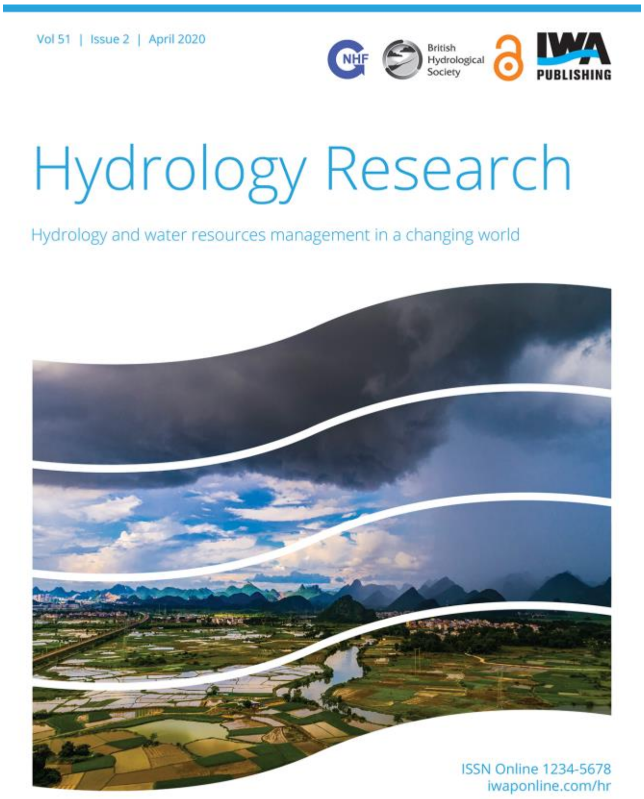

Risk assessment for areas prone to flooding and subsidence: a case study from Bergen, Western Norway

Guri Venvik, Ane Bang-Kittilsen and Floris C. Boogaard

ABSTRACT

Bergen city centre is prone to both subsidence and flooding. With a predicted increase in precipitation due to climate change, a higher proportion of rainfall becomes surface runoff, which results in increased peak flood discharges. In addition, it has been predicted that sea-level rise and increasing storm surges will result in coastal flooding. In this study, the dual hazards of flooding and subsidence are analysed to exemplify possible risk assessment maps for areas most prone to the combination of both. Risk assessment maps are a support tool to identify areas where mitigation of subsidence and adaptation for surface water management will be most efficient and measures can be implemented. The results show that dual hazard assessment, like that described in this paper, can be a useful tool for decision-makers when prioritizing areas to implement measures such as Sustainable Urban Drainage Systems.

Key words | flooding, groundwater, InSAR, risk assessment, subsidence, surface water

Guri Venvik (corresponding author)
Ane Bang-Kittilsen
Geological Survey of Norway (NGU),
P.B. 6315 Torgarden, 7491 Trondheim,
Norway
E-mail: *guri.venvik@ngu.no*

Ane Bang-Kittilsen
Faculty of Engineering, Department of Civil and Environmental Engineering,
Norwegian University of Science and Technology,
Trondheim,
Norway

Floris C. Boogaard
NoorderRuimte, Centre of Applied Research and Innovation on Area Development, Hanze University of Applied Sciences,
Zernikeplein 7, P.B. 3037, 9701 DA Groningen,
The Netherlands

INTRODUCTION

It is expected that 60% of the world's population will be living in urban areas by 2030, and most of this area has yet to be built (UN 2016). The pace of urban growth may be overwhelming and exert tremendous pressure on the catchment hydro(geo)logy in general and urban drainage in particular (Marsalek *et al.* 2006). The built urban infrastructure, with asphalt and concrete-covered ground surfaces, alters hydrologic abstractions and water flow found in natural catchments (Bolund & Hunhammar 1999). It has been predicted that climate change will increase precipitation (Hanssen-Bauer *et al.* 2017), and a higher proportion of rainfall will become surface runoff, which, in turn, will result in increased peak flood discharges and degraded water quality (Haughton & Hunter 1994). In addition, the sea level is predicted to rise by up to 1 m by 2090 (Hanssen-Bauer *et al.* 2017). Changes in the urban environment due to growth in addition to climate change put the urban water cycle out of balance, thereby affecting other surface and subsurface processes, such as flooding and subsidence.

Urban areas are, to a large extent, built environments, and from that view constitute a unique environmental challenge. As Pregnolato *et al.* (2017) point out, cities are particularly vulnerable to flooding and rapid and intense rainfall due to the impermeable surfaces that dominate areas with high concentrations of people, buildings and infrastructure. As a result of the increasing flood damage in Europe, there has been a shift in attention from flood protection to flood risk management (Albano *et al.* 2018), where risk assessment with tools, such as maps, are central. This

doi: 10.2166/nh.2019.030

shift is also valid for risks other than flooding, such as subsidence.

Both pluvial and coastal flooding can be related to subsidence (Dixon *et al.* 2006; Miller *et al.* 2008; Yin Yu & Wilby 2016). For the Bryggen Wharf, in central Bergen, western Norway, there is a strong link between water and subsidence, due to reduction in water in the subsurface cultural layers, as well as lowering of the groundwater levels leading to the decay of organic layers as well as historical wooden foundations and thereby subsidence (de Beer *et al.* 2012; de Beer & Seither 2015; Matthiesen *et al.* 2015; Rytter & Schonhowd 2015b). Other geological processes commonly linked to subsidence include tectonic structures, land and rock slides, gravitation (Berardino *et al.* 2003; Lauknes *et al.* 2010; Eriksen *et al.* 2017) and subsidence due to groundwater depletion (Chaussard *et al.* 2014; Castellazzi *et al.* 2016; Motagh *et al.* 2017).

In order to provide communities with urban infrastructures that are durable and well-functioning, climate change impact and adaptability assessments are vital (Pregnolato *et al.* 2017). Flood modelling is a useful tool for planning floodways, identifying areas for mitigation measures and for bringing awareness of water issues into decision-making processes in urban areas (Fletcher *et al.* 2013; Albano *et al.* 2017; Boogaard *et al.* 2017a, 2017b; Lyu *et al.* 2018). Hence, risk assessment mapping can be further used for identifying areas for the implementation of Sustainable Urban Drainage Systems (SuDS), such as swales, to infiltrate water into the ground and to sustainably manage surface water in urban areas. More knowledge is needed to understand the urban water balance and the processes connected to water to prevent and counteract subsidence that can cause damage and unforeseen expenses.

Increased knowledge and understanding of the urban water cycle in the transitional zone between the built and natural environment is necessary. In the case of Bergen city centre, past research has shown that the subsidence to a large degree is driven by the depletion of water in the underlying organic-rich cultural layers (Harvold *et al.* 2015; Matthiesen *et al.* 2015). For a complete understanding of the urban water cycle, hydrological and hydrogeological studies should be included (Wakobe *et al.* 2018). Hence, we combine datasets for flood risk and subsidence to develop a risk assessment map for areas prone to damage. The case study is set in Bergen city centre (Figure 1), on the west coast of Norway. Bergen is a coastal city where the annual precipitation is high, 2,250 mm/year (NMI 2019). The city is therefore prone to water-related damage caused by pluvial flooding, storm surges and stormwater flooding.

The subsidence data are computed using satellite-based persistent scatterer interferometry (PSI; Crosetto *et al.* 2016). PSI has long been used to compute subsidence, especially related to groundwater depletion (e.g. Schmidt & Bürgmann 2003; Teatini *et al.* 2012). In this study, data from the Sentinel-1 satellites have been used as an input. Further, subsidence data have been correlated with an LiDAR DEM (Norwegian Mapping Authority 2009)-based urban flood model result.

Dual hazard analyses have been carried out by two different analysis methods using ArcGIS (ESRI 2018). In both methods, the resulting map is a grid, which is a common areal unit when synthesizing multiple variables (Carver 1991; Damoom *et al.* 2019). The first method is a simple grid overlay, recording the occurrence of input data within the grid cells. The second method uses Getis-Ord G* statistics (Getis & Ord 1992) commonly called 'hot spot analysis' (ESRI 2019), which automatically detect clusters of incident data within the bounding area of flood data. As an example, Lu *et al.* (2012) use the 'hot spot analysis' to detect slow-moving landslides from InSAR data. Geographical Information System (GIS)-based analysis for risk assessment is widely used to investigate various hazards, such as flooding (Albano *et al.* 2017, 2018; Lyu *et al.* 2018) and for multi-criteria decision-making analysis (Erbaş *et al.* 2018; Damoom *et al.* 2019). As pointed out by Damoom *et al.* (2019), when combining different datasets GIS allows the user to visualize, inquire, analyse and interpret the vast amount of (geological) data for a better understanding and problem-solving. Therefore, the risk assessment analysis presented in this paper aims to identify areas prone to the dual hazards of both flooding and subsidence. Dual hazard assessment maps, based on existing flooding and subsidence data, were executed using overlay and 'hot spot' analysis in the GIS. Results can be used as a tool to select areas that need mitigation and damage prevention measures, both for buildings and urban infrastructure. Risk assessment, shown in this case study, may be applied in urban (or rural) areas where data, such as subsidence and flooding, are available.

Figure 1 | Bergen city centre viewed towards the southeast with steep hillside and lower lying area along the shoreline (Google Earth, 2019). Please refer to the online version of this paper to see this figure in colour: http://dx.doi.org/10.2166/nh.2019.030.

STUDY AREA AND DATA

Bergen is the second-largest city in Norway, located on the west coast, with an area of 464 km^2 and a population of 278,556 (SSB 2017). The city has an annual average temperature of 8.6°C and an annual precipitation of 2,250 mm (NMI 2019). The climate is predicted to become wetter with more intense and frequent downpours, which will increase the pressure on surface water runoff and stormwater management (Hanssen-Bauer *et al.* 2017). The topography of Bergen city centre, as well as the surrounding areas, encompasses steep hillsides covered with forest vegetation on thin soil cover, down to flat-lying former shorelines with thicker natural sediments and anthropogenic layers. A 1 km relief goes from Fløyen (at 320 m a.s.l.) to Bryggen (at 1 m a.s.l.) (Figure 1). These natural conditions make surface runoff water abundant.

The study area has been constrained to the city centre, including the Medieval city and its surrounding area. In the city centre, the anthropogenic cultural heritage layers are thick with a rich organic content locally more than 10 m thick (Figure 2). The old shoreline from the 12th century (Hansen 1994) is shown in Figure 2. Since Bergen has close to no isostatic land uplift (Mangerud 2004), the progressing

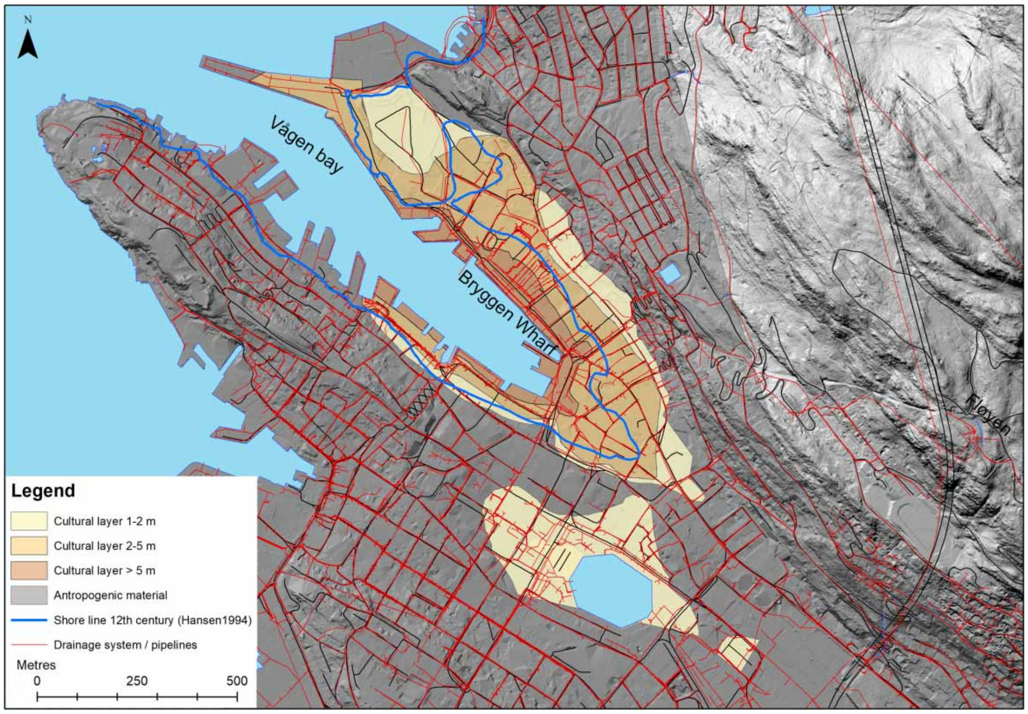

Figure 2 | In Bergen city centre, the subsurface consists of exposed bedrock in the hillside (light grey colour), anthropogenic material (dark grey colour) and up to 10 m of cultural layers (brown colour), on top of beach sand, clay and till before reaching bedrock below. (Directorate for Cultural Heritage, 2018, Norwegian Map Authority, 2018). Please refer to the online version of this paper to see this figure in colour: http://dx.doi.org/10.2166/nh.2019.030.

shoreline of today is due to filling of the anthropogenic material such as waste into the bay area, Vågen. These layers are more prone to destruction due to lack of infiltration of surface water; therefore, the Bryggen project was initiated in 2010 to save the UNESCO World Heritage site of the Hanseatic League Wharf (Ersland 2015; Rytter & Schonhowd 2015a). Rytter & Schonhowd (2015a) document the connection between soil moisture, groundwater level and the decay or preservation of organic anthropogenic material. The lack of soil moisture and very low groundwater levels can lead to the higher oxygen concentration in the organic matter and acceleration of disintegration. The organic layers then collapse and compact (Matthiesen *et al.* 2015), resulting in subsidence of the ground and damage to buildings and infrastructure (Jensen 2015; Rytter & Schonhowd 2015b). Bryggen is an example where measures have been taken by implementing SuDS to infiltrate surface water into the subsurface to increase soil moisture and groundwater level and thereby preserve the cultural layers and stabilize the ground (de Beer *et al.* 2012; Boogaard 2015; de Beer & Seither 2015).

Drainage system in Bergen city

To handle the surface water and stormwater, Bergen city has a drainage system with the purpose of transporting water effectively out of the city. In the greater parts of the city, especially in the inner centre, the stormwater is brought together with the wastewater from the industry and household (Figure 2; Bergen Kommune 2006). When intense rainfalls occur, the capacity of the drainage system is strained, which may cause the emission of wastewater. Since the relief in the city centre is steep (Figure 1) and the surface has low permeability, flooding arises when large and intense rainfalls occur in short time spans. Due to climate change, events with downpour will be more intense and frequent. This, in addition to predicted sea-level rise, will give more frequent and intense flooding where there are topographic depressions (Hanssen-Bauer *et al.* 2017), as seen in Figure 3.

For this study, we included a dataset of the pipelines for wastewater and sewage. It should be noted that the sewage system may be a combined stormwater and sewage, or a

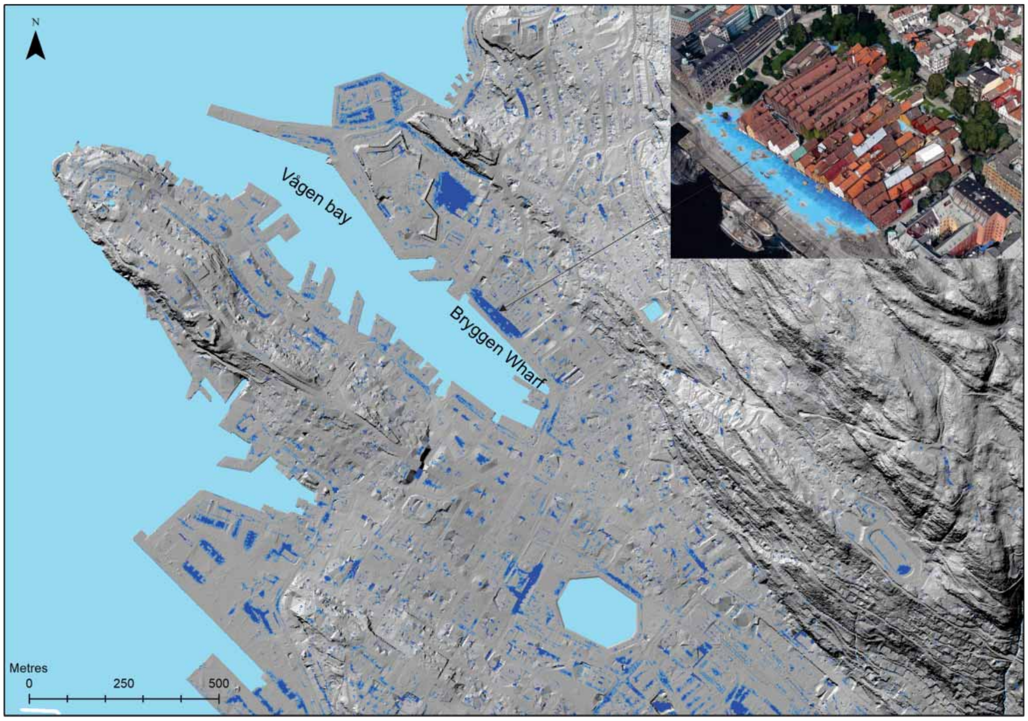

Figure 3 | Pluvial flood model result of Bergen city based on DEM and rainfall input, where terrain and depressions control the flow path and accumulation of surface water. Increase in colour intensity with the increasing surface water depth. The inserted photo shows the area in front of Bryggen Wharf prone to pluvial flooding. Please refer to the online version of this paper to see this figure in colour: http://dx.doi.org/10.2166/nh.2019.030.

separate system: these are not differentiated in the dataset (Bergen Kommune 2006).

Flood modelling

Pluvial, urban flooding has received increased attention over the last decade (Mignot *et al.* 2019), due to the costly damage on infrastructure and society (Miller & Hutchins 2017; Sörensen & Mobini 2017). There are many tools for urban stormwater flood modelling as pointed out by Balstrøm & Crawford (2018), which have been improved after the July 2011 Copenhagen event with close to a 100 mm/h rainfall (Miller & Hutchins 2017; Sörensen & Mobini 2017; Mignot *et al.* 2019). The flood modelling itself is not the scope of this work but the dual hazard of flooding and subsidence. The flood map was created as a case study of Bergen in the INXCES project described in Boogaard *et al.* (2017a, 2017b), and the results are further used for analysis in this study. The urban flood modelling was created using the Calamity Levels of Urban Drainage Systems (CLOUDS by Tauw bv) method with the aim of modelling and simulating water flow and water accumulation (Kluck *et al.* 2010; Boogaard *et al.* 2017a, 2017b, 2018). The simulation was run with a precipitation of >60 mm/h, where 20 mm/h is estimated to run in the sewer system and 40 mm/h on the surface. This represents an extreme storm or a 100-year event (Kluck *et al.* 2010, 2015). With this assumption, the digital elevation model (DEM; Norwegian Mapping Authority 2009) and rainfall distribution serve as the main input. The flood simulation was done to increase the understanding of which urban areas are most prone to flooding as well as indicating runoff flow paths for surface water (Figure 3). The Bryggen Project is a best management practice that demonstrates the linkage between infiltration of surface water, recharge of groundwater, preserving cultural layers and preventing subsidence (de Beer *et al.* 2012; Boogaard 2015; de Beer & Seither 2015; Matthiesen *et al.* 2015; Rytter & Schonhowd 2015a). This flood simulation indicates areas where infiltration of surface water will be most advantageous with regard to reducing flooding as well as subsidence. This can further be used to plan floodways for the city.

The resulting map shows stormwater accumulation, where the darkest blue colour indicates a greater water depth (Figure 3) (the colour figure can be viewed online). The DEM was created from LiDAR data produced from the FKB-Laser (Felles KartdataBase/common map database) dataset consisting of 1 point per m^2 (Norwegian Map Authority/Kartverket 2009). A detailed description of method, calculations and results from the flood modelling is presented in Boogaard *et al.* (2017a) and Kluck *et al.* (2010). For a complete comprehension of the urban water balance, hydrological and hydrogeological studies should be included (Wakode *et al.* 2018).

Present-day storm surge

In November 2018, the Norwegian Mapping Authority launched an open access web service with models of current and future (2090) sea-level rise and storm surges. The data, map tool and services are aimed at the planning of coastal areas (DSB 2017). The storm surge height intervals are mean high water, 20-year, 200-year and 1000-year return periods. One of the Mapping Authority's datasets entitled '200-year storm surge' (Figure 4) shows sea level under these extreme conditions. In Bergen, there are small differences in sea-level heights for the different return periods of storm surges (https://www.kartverket.no/sehavniva/). The dataset for present-day 200-year storm surge was chosen as the most relevant occurrence for further analysis and was incorporated into the dataset of pluvial flood for further use (Figure 4). Some of the pluvial flooded areas (Figure 3) coincide with the storm surge flooded areas.

Subsidence data

The subsidence data used in this study were produced by the Norwegian Ground Motion Service (Figure 5; www.insar.no). Using radar images from the Copernicus Programme's Sentinel-1 satellites, the service provides over two billion deformation measurements over the entire Norwegian mainland. At each point, both the average velocity (along the satellite-to-ground line-of-site) and a cumulative deformation time series are provided. The Sentinel-1 satellites provide full coverage of Europe every 6 days. The wide acquisition swath (250 km), along with Norway's northern

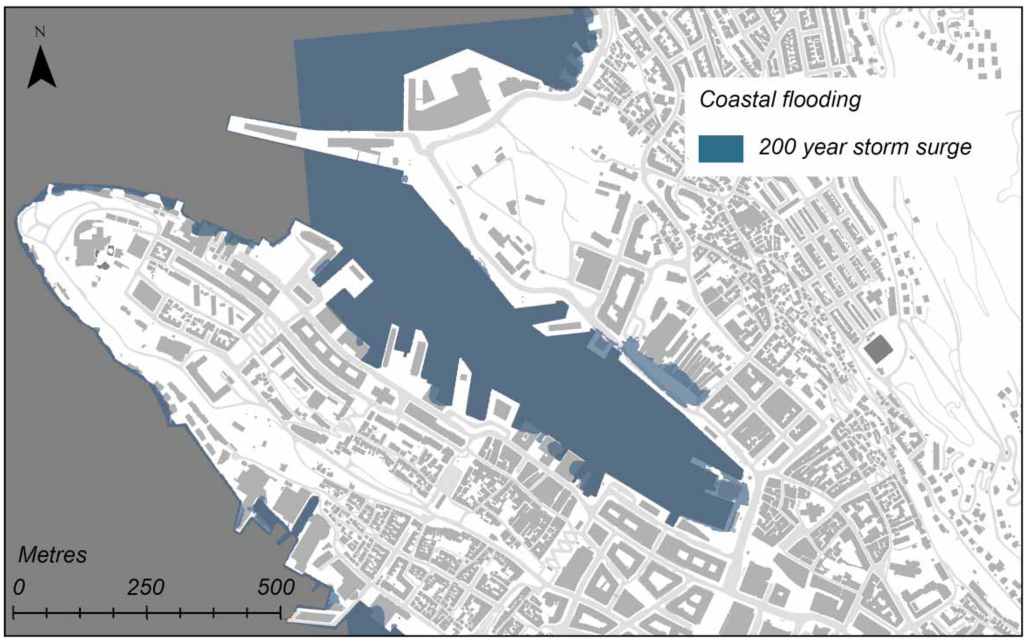

Figure 4 | Areas prone to coastal flooding during a 200-year storm surge are indicated with blue areas on land. Data from the Norwegian Map Authority (2018) (https://www.kartverket.no/sehavniva/). Please refer to the online version of this paper to see this figure in colour: http://dx.doi.org/10.2166/nh.2019.030.

Figure 5 | PSI data from Sentinel-1 for the time period 2015–2018 collective ground movement, subsidence (vertical velocity) in mm/year. Data from the Norwegian Map Authority (2018). Please refer to the online version of this paper to see this figure in colour: http://dx.doi.org/10.2166/nh.2019.030.

latitude, results in multiple overlapping datasets for each area on the ground. For this study, four independent datasets were used, two from ascending (north-going) orbits and two from descending (south-going) orbits. The input data cover the time period 2015–2018, where two datasets are from 2015 to 2018, while two datasets are from 2016 to 2018 (Figure 5). Only data from June to October were used to reduce the possible effects of snow cover. The PSI technique does not return any data from vegetated areas. In the built environment, datapoints commonly represent buildings and other surface constructions.

One advantage of multiple, independently processed PSI datasets is that they can be compared with each other as a basic quality control step. In our study, the datasets were self-consistent. For a smaller area, at the site of the Hanseatic Wharf 'Bryggen', the PSI data have been controlled by comparison with ground-based monitoring of movement (Jensen 2004, 2015; Haukedal 2017). These studies show that both measuring techniques reveal similar patterns of movement and the order of subsidence within the same time period. However, ground-based measurements are time-consuming and costly compared to satellite data collection.

For this study, a threshold for the PSI data was set to −1 mm, only negative vertical movement, subsidence, from −1 mm and larger was included. All data with values 0 mm or more, positive (+) vertical movement was discarded.

METHODOLOGY – RISK ASSESSMENT APPROACH

The Geographical Information System tools such as ArcGIS and ArcGIS Pro (ESRI 2018) were used for the analysis in this study, with the aim of detecting areas with a risk of both subsidence and flooding. To prepare the datasets for analysis, the results from the flood model were georeferenced and vectorized and clipped against the shore. The original flood model consisted of many small and scattered polygons. Since the focus was on areas with severe flood problems, flood polygons spaced closer than 3 m were aggregated, while the areas smaller than 10 m^2 were removed. Then, the results from the pluvial flooding were merged with the 200-year storm surge data. Only PSI points with more than 1 mm/year subsidence were used (Figure 5). The uncertainties connected with these datasets will be discussed later.

The first and simplest overlay is a plain visual overlay of the input data, showing flood data (blue areas in Figure 6(a)) with subsidence data (red points in Figure 6(b)) on top (Figure 6(c)) (the colour figures can be viewed in the

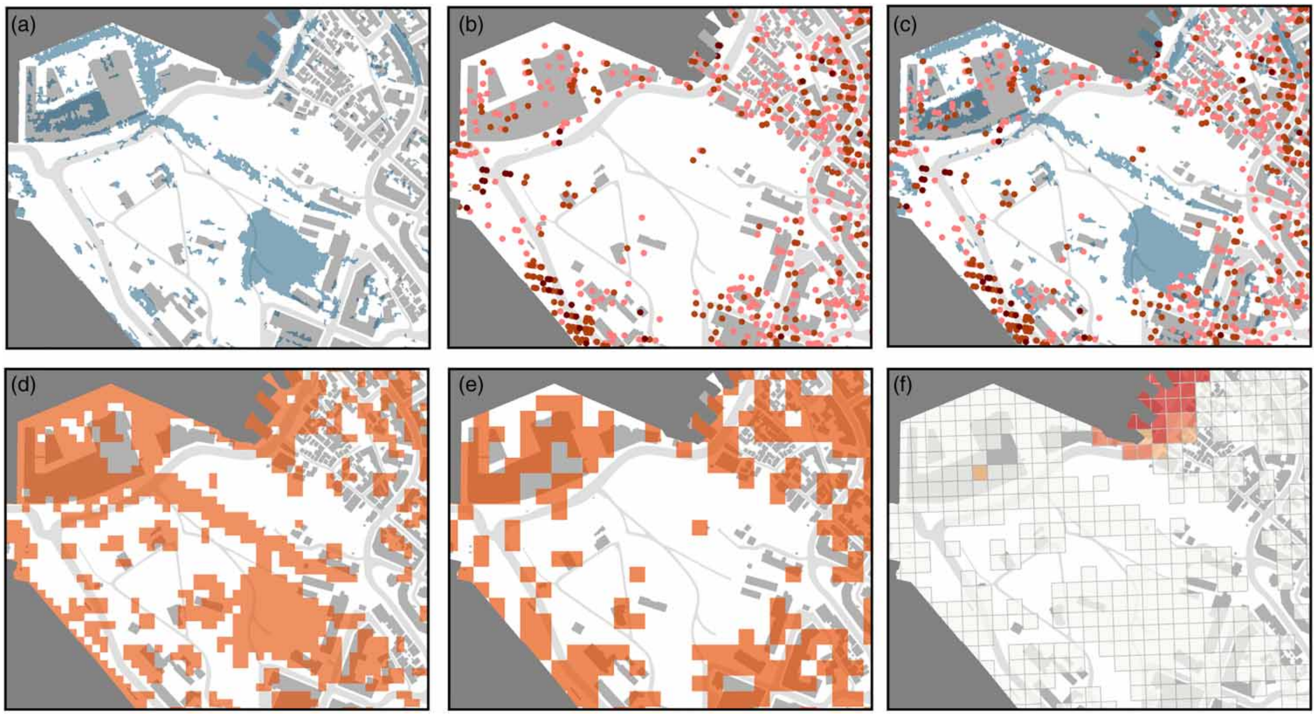

Figure 6 | Top row: the datasets used in the analysis: (a) flooding, (b) subsidence and (c) the combination of the two datasets. Bottom row: results from methods. (d) Method 1 with grid cells with 10 × 10 m, (e) method 1 with 20 × 20-m grid cells and (f) method 2, the 'hot spot analysis' of subsidence within the flooded area. This method uses 20 × 20-m grid and the three different colours displaying 90%, 95% and 99% confidence levels. Please refer to the online version of this paper to see this figure in colour: http://dx.doi.org/10.2166/nh.2019.030.

online version of the article). A visual overlay is useful both to evaluate results from automatic tools and as a complementary map for detailed insights. For planning purposes, pre-selecting areas for action lead to more effective decision-making (Campbell *et al.* 2017; Hooimeijer *et al.* 2017; Hanssen 2018). This work uses grids to synthesize the input data. Grid maps reduce the degree of detail and are expected to give the impression of data uncertainty because it clearly does not follow the pattern of flooding nor the built infrastructure. Two methods were used (Figure 6): The first method does not take the spatial clustering of subsidence into account (Figures 6(d) and 6(e)). The second method analyses the clustering of subsidence within areas prone to flooding (Figure 6(f)).

Description of the simple grid overlay method (1)

In the first method, grids of different sizes are created followed by a selection of grid cells that cover areas with a risk of both flooding (Figure 6(a)) and subsidence (Figure 6(b)). See Figures 6(d) and 6(e) for selected areas, respectively, for grids of 10 × 10 m and 20 × 20 m. The method followed two manual operations:

(I) Two different grids were made with grid size set to 10 × 10 m (Figure 6(d)) and to 20 × 20 m (Figure 6(e)). The flood data map extent was used as the template extent. (II) Grid cells containing both flood and subsidence data are given the colour orange in the map, as shown in Figures 6(d) and 6(e).

Description of the 'hot spot analysis' with aggregated flood areas method (2)

This method uses the optimized 'hot spot analysis' tool to create a grid showing hot spots of subsidence data within areas with a risk of flooding (Figure 6(f)). This tool uses the Getis-Ord Gi* statistic to identify statistically significant hot spots (ESRI 2019). For this method, we went through the following parameters: the main input was the subsidence data and grid cells of 20 × 20 m were selected. Aggregation was selected to count incidents of subsidence within the grid cells within areas prone to flooding. The result was a map with grid cells showing statistically significant hot spots of subsidence that also are at risk of flooding, as shown in Figure 6. A visual comparison of the results with the cartographic overlay as shown in Figures 6(c) and 7 was done to ensure that the areas with the highest values of subsidence were represented.

RESULTS AND DISCUSSION

The areas identified to be at dual risk in this study could further be targeted for mitigation measures that allow surface water to infiltrate the subsurface. Firstly, such measures would help maintain the anoxic conditions necessary to impede the decay of the rich organic layers. Secondly, mitigation measures could help stabilize the groundwater levels and assist in preventing further subsidence. Participants of the Bryggen Project demonstrated that the groundwater levels could be stabilized by introducing SuDS for retaining, storing and further infiltrating surface water (de Beer *et al.* 2012; Boogaard 2015; de Beer & Seither 2015; Matthiesen *et al.* 2015; Rytter & Schonhowd 2015b; Boogaard *et al.* 2016). Large areas of impermeable surface in the city centre also contributed to the risk of flooding. Natural water management practices, like the implementation of SuDS, help increase the infiltration of floodwater to subsurface soils and groundwater. This study gives an example from Bergen city but is relevant for cities having similar challenges related to flooding and subsidence.

Datasets and selected methods for analysis

A visual analysis of the input data reveals an image of a city widely affected by subsidence and flooding after heavy rainfall or storm surges, as shown in Figure 7. To make visual analysis easier, the PSI data are shown with points of increasingly darker red for higher degrees of subsidence (the colour figures can be viewed in the online version of the article). The flooded areas are shown in blue. Areas most prone to flooding and subsidence become prominent in this visualization (Figure 7).

Subsidence data

It should be noted that PSI datapoints may represent points on the ground or points on the city infrastructure,

Figure 7 | The PSI data indicates that subsidence is shown in red and the flooded areas in blue. With an overlay of the two datasets, the map shows a city widely affected by subsidence as for areas prone to flooding. Please refer to the online version of this paper to see this figure in colour: http://dx.doi.org/10.2166/nh.2019.030.

such as buildings. Any hard object on the surface may reflect a signal. As such, there is always the possibility that individual points are measuring the deformation of the city infrastructure or in the building itself, and not ground subsidence. Additionally, the PSI technique does not return any measurement in vegetated areas, such as yards or parks. Nonetheless, more than 300,000 datapoints were used in this study providing orders of magnitude more information than could have been obtained using traditional surveying techniques. Although there are many historic buildings in the area, most have been rehabilitated in the last decade and we do not expect that building deformation is a significant part of what is measured. Therefore, we have great confidence that PSI data are suitable for the risk assessment. In this study, all PSI points with more than 1 mm subsidence are included. The exact value of vertical velocity is not used in either of the analyses, only the presence in the simple grid overlay (method 1, Figure 8) and the cluster of points in the 'hot spot analysis' (method 2, Figure 9). For method 2, a visual control of the result shows that areas of high value are also selected as hot spot areas.

Flood data

Results from the urban flood modelling, used in this study, emphasize the areas prone to flooding (Boogaard *et al.* 2017a). The flood modelling is based on the DEM and on the rainfall distribution where depressions in the terrain will control the flooded areas. Manmade constructions, including roads, will create sinks where the flooding will occur (Kluck *et al.* 2010, 2015; Boogaard et al. 2017a, 2017b; Balstrøm & Crawford 2018). For the flood results presented here, this is regarded as inevitable because the study is in an urban and built environment.

Planners are interested in surface water flood modelling and simulation at a coarser and more overall level (Balstrøm & Crawford 2018) for the purpose of prioritizing and decision-making (Campbell *et al.* 2017; Hanssen 2018). For a complete flood risk assessment analysis, hydrological and hydrogeological studies (Wakode *et al.* 2018), an updated flood model, based on an updated DEM, topographic data and flow parameters should be included. The flood risk due to storm surge is based on the estimated highest level of storm surge at present day (Norwegian Mapping Authority; www.Kartverket.no). The storm surges are

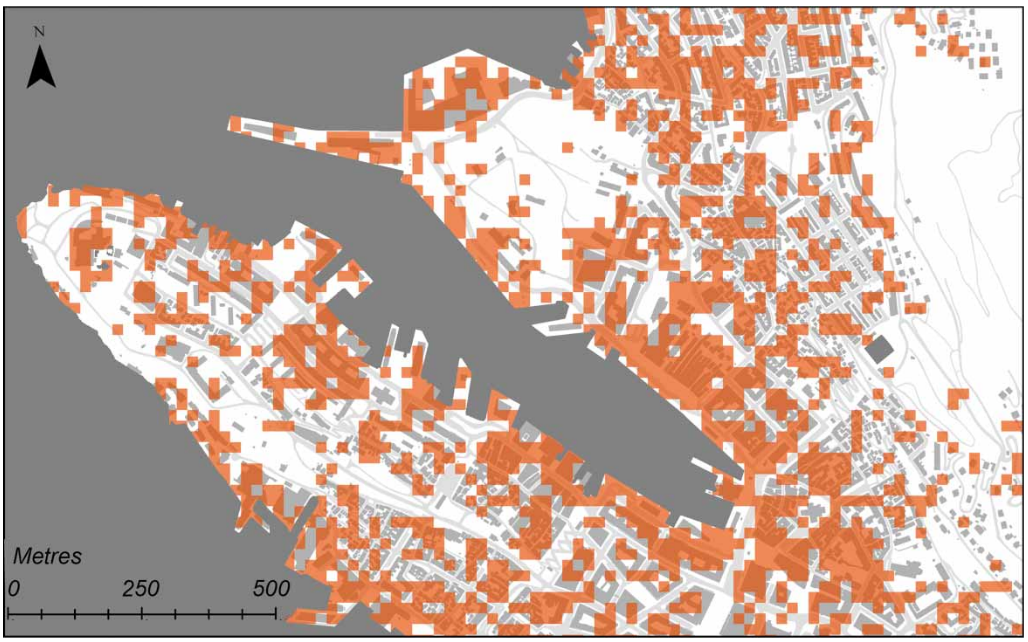

Figure 8 | Simple overlay analysis with 20 × 20-m grid shows where both subsidence and flooding occur. Please refer to the online version of this paper to see this figure in colour: http://dx.doi.org/10.2166/nh.2019.030.

modelled with 20-year, 200-year and 1000-year intervals (Map Authority). For Bergen city centre, the differences are minor. The 100-year design precipitation (Kluck *et al.* 2010, 2015) for the pluvial flooding is therefore combined with a 200-year storm surge, as an extreme event. In further steps for risk assessment, this dataset should be updated and include the worst-case scenario of sea-level rise (IPCC 2014).

Simple grid overlay – method 1

For the simple grid overlay with grid sizes of 10×10 m and 20×20 m, the result is numerous small areas as shown in Figure 8. It is clearly illustrated in the case of the city centre that a simple grid overlay method gives minimal guidance for authorities as to which areas should be prioritized for dual hazard mitigation. Due to the characteristics of the two datasets; flooded areas in streets and PSI data on buildings and grid cells of 10×10 m and smaller give a result of scattered patches and no area of significance. However, when the grid cells are 20×20 m, areas prone to both flooding and subsidence are distinguished, as shown in Figure 8.

'Hot spot analysis' - method 2

The hot spot analysis, method 2, does the narrowest selection of areas, using the aggregated flood data and a count of subsidence hot spots within each 20×20 m grid cell (Figure 9). The results show that within our study area, there are several areas of significance. For a decision-making process, it would be easier to prioritize areas for mitigation using the 'hot spot analysis' for risk assessment mapping, as shown in Figure 9.

Risk assessment map combined with the existing drainage system

As an example of usability, the risk assessment maps from the simple overlay analysis (method 1, 20×20 m grid cells) and the 'hot spot analysis' (method 2) have been combined with the existing drainage system. A 'near-analysis' with 3 m radii of areas in dual hazard and pipelines intersect shows areas where the drainage system is under great pressure when heavy and rapid rainfall or a storm surge occurs (Figure 10). This is standard procedure within water management (Marsalek & Chocat 2002; Marsalek *et al.* 2006). However, this study shows the connected drainage pipes

Figure 9 | 'Hot spot analysis' where clusters of subsidence are within areas of pluvial or coastal flooding. The grid cells are 20×20 m. Please refer to the online version of this paper to see this figure in colour: http://dx.doi.org/10.2166/nh.2019.030.

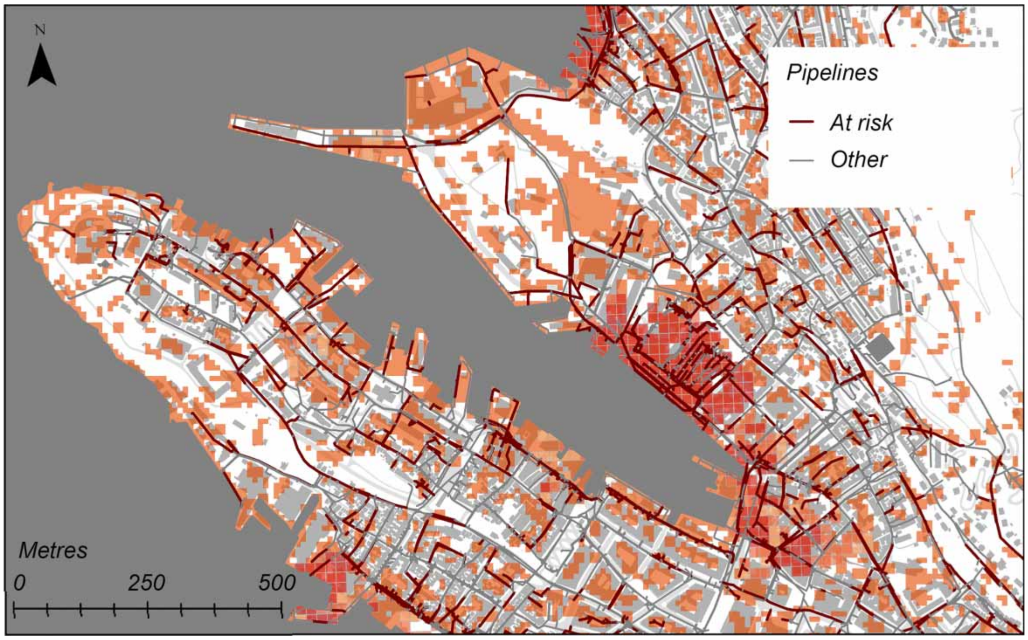

Figure 10 | A 'near-analysis' of pipelines shows all pipes affected by both subsidence and risk of flooding within 3 m distance (red lines). The results from the simple overlay analysis (method 1) with 20 × 20-m grid cells and the 'hot spot analysis' (method 2) are included in the map. Please refer to the online version of this paper to see this figure in colour: http://dx.doi.org/10.2166/nh.2019.030.

and manholes that in addition to high water pressure and excess surface water are prone to ground subsidence that may cause damage and disconnect the pipes (Figure 10). In these areas, it is expected that the drainage system has a greater need for maintenance and thereby costs.

Figure 11 compares all methods, where (A) displays the raw data where blue colour shows flooding and red colour shows subsidence (the colour figures can be viewed in the online version of the article). This visualization indicates that the larger parts of the city are influenced by flooding or subsidence, or both. Comparing the two methods: (1) simple grid overlay and (2) 'hot spot analysis' (Figure 11), the best choice of the method depends on the end-use. Method 1 uses input data raw and has no regard to the size of areas flooded or the density or degree of subsidence. Consequently, the result for Bergen marks areas on almost all buildings in the study area (Figures 8 and 11(b)). When using small grid sizes and without consideration of nearby objects, there is a risk of overlooking relevant areas. There is no prioritizing, and one can argue whether this map result is of any benefit to Bergen's decision-makers other than seeing that there are large areas of dual hazard. It may also contribute to a loss of information due to the cartographic overlay of the input dataset (Figure 11(a)). Nonetheless, the result does suggest that there is a need for general guidelines for city management and building owners. At this level of detail, and if the target user group was property owners, the method can focus on buildings that are prone to flood and subsidence. A 'near-analysis' would possibly be a better alternative as exemplified with pipelines in Figure 10. The results from the 'hot spot analysis' (method 2) are more selective and areas are clearly prioritized (Figure 11(c)). For scientific research on the relationship between flooding and subsidence, or for the municipality to select areas for greater follow-up, this method gives significant results for the clearest selection of areas (Figures 9 and 11).

Risk assessment as a tool for end-users

Subsidence in urban areas is often related to water. A lack of water in the subsurface may lead to compactions of sediments and where organic matter is present, decay and decomposition (Chaussard *et al.* 2014; de Beer & Seither 2015; Matthiesen *et al.* 2015; Castellazzi *et al.* 2016; Motagh *et al.* 2017). Excess water causes flooding and increased erosion (Dixon *et al.* 2006; Miller *et al.* 2008; Yin *et al.* 2016).

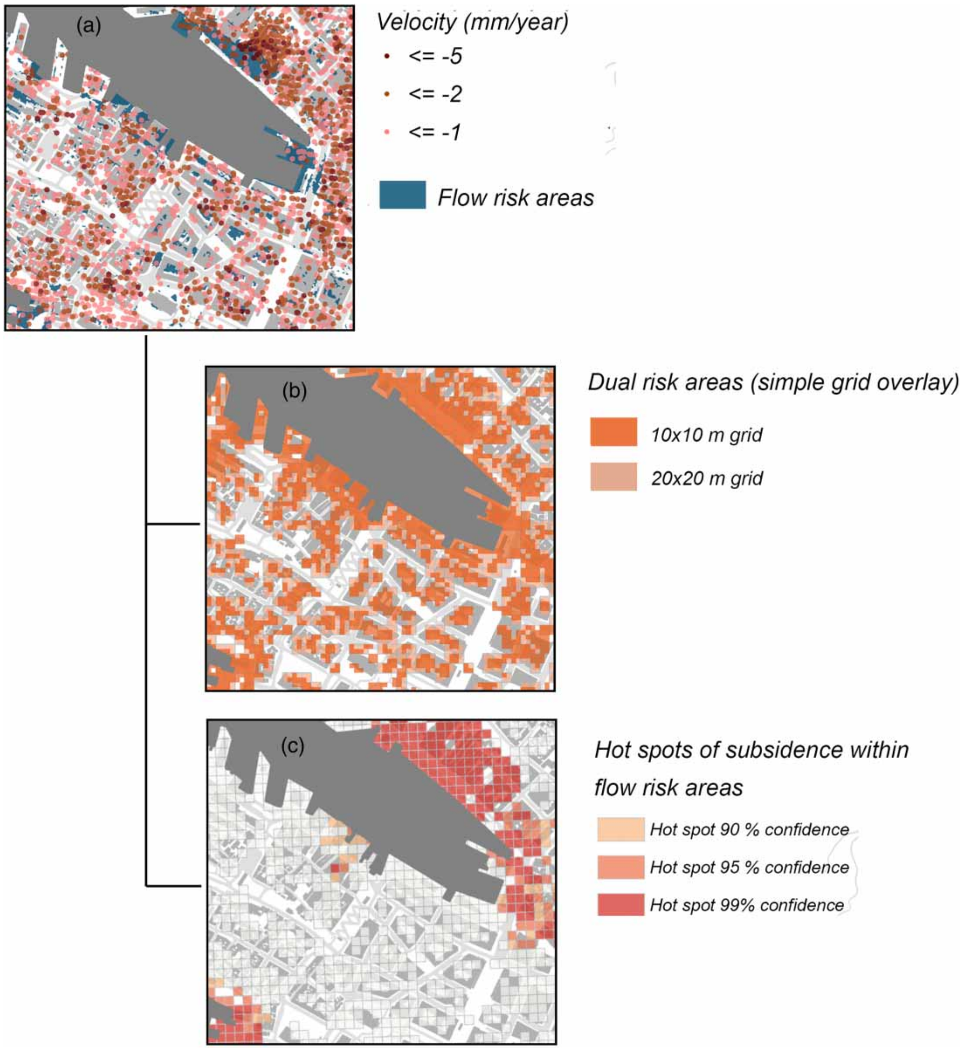

Figure 11 | Comparing the methods. (a) The input data are shown in blue for flooded areas and red for subsidence by PSI data. (b) In method 1, the 10 × 10 (dark orange colour) and 20 × 20 (light orange colour) metre grid cells are all containing both flood risk and subsidence. (c) In method 2, fewer areas are selected based on a 'hot spot analysis' on subsidence bounded by the existence of aggregated flood data. The colour nuance reflects 99%, 95% and 90% confidence levels as displayed in Figure 9. Please refer to the online version of this paper to see this figure in colour: http://dx.doi.org/10.2166/nh.2019.030.

The subsurface of any city is complex, and in Bergen, it can be roughly divided into three layers: natural ground consisting of bedrock and sediments on top, cultural layers consisting of domestic waste, with up to 100% organic matter (Matthiesen *et al.* 2015; Rytter & Schonhowd 2015b) and anthropogenic materials, such as agglomerate, asphalt and material for drainage. The subsidence occurring is not constrained by geological structures and cannot be explained by geological processes alone. However, water, both surface water and groundwater, plays an important part in the process.

Pregnolato *et al.* (2017), in their risk assessment of roads in Newcastle, UK, show that roads are prone to flooding during heavy rainfall. Similarly, the risk assessment presented in this study can help the municipality prioritize areas for mitigation or that need on-going surveillance. A current discussion in Norway is how to implement climate adaptation into best management practice for municipalities (Hanssen 2018). Hanssen (2018) shows how well flood risk maps function to translate natural science information into local planning and decision-making. This shows that maps are credible and essential tools, but that they need to be brought to the table by planners and interpreted in a local context. Hanssen (2018) conclude that local climate adaption is dependent on well-functioning interaction between multiple levels as well as disciplines and emphasis on strengthening the role of the government agencies as 'knowledge translators' ('kunnskapsoversettere'; Hanssen 2018). The risk assessment map methodology presented in this study aims to translate knowledge into maps to assist the end-user to select areas for implementation of, for example, SuDS by identifying areas prone to the dual hazard of flooding and subsidence. Resilience of the built environments has not been well studied (Thornbush *et al.* 2013), and results from this study may help the Bergen Municipality to plan mitigation and further adaptation to prevent areas of flooding, by increasing infiltration of surface water and decreasing flooding, as well as the processes causing subsidence. Managing stormwater is not just important for protecting water resources and aquatic ecology but also to restore urban water cycle processes that are critical to the health of urban watersheds. These include infiltration and groundwater recharge, evapotranspiration and chemical/biological transformations, especially due to more frequent and intense rainfall and flooding (UN-Water 2018).

CONCLUSIONS

There is a link between areas that suffer from subsidence and areas with an excess or shortage of water. The aim of this study was to locate areas in Bergen city centre that are prone to the dual hazard of subsidence and flooding. This was achieved by processing existing data and maps that identify areas prone to PSI data for risk of subsidence, a flood model map and a storm surge map for areas prone to flooding.

We have demonstrated that a 'hot spot analysis', for the subsidence data within areas prone to flooding, provides an effective means of selecting areas for further field evaluation. Data for climate adaptation analyses are increasing and open access. The method can easily be repeated with updated PSI and flood data. The areas selected are constrained and could serve as a starting point in prioritizing areas by the municipality for detailed hydrological and hydrogeological studies of the urban water cycle and further implementation of water management solutions, like SuDS.

The subsurface in cities is complex due to a mixture of natural and built environments. The processes causing subsidence are not easily understood but are commonly related to water. Increasing infiltration of surface water may prevent the processes causing subsidence. Managing stormwater in this way is not only important for protecting water resources and the aquatic environment – it can help restore and maintain urban water cycle processes critical to making cities resilient to the effects of climate change.

Further work

The increased availability of data, both large datasets and timeseries, makes analyses, such as the risk assessment presented here, much more achievable. The Copernicus program is revolutionary in that it promises this type of data for decades to come, free and open. Risk assessment similar to that conducted in this study is relevant for all cities that are prone to coastal and/or pluvial flooding or possible the combination of flooding and subsidence. The www.InSAR.no service is an open access portal, displaying data used in this study, and is an example of possibilities with the upcoming EU Ground Motion Service.

The latest available PSI data and a new and updated flood model based on the latest and most detailed DEM and topographic data should be used before selecting areas in a potential follow-up of this study. This risk assessment should be also followed up by hydrological and hydrogeological field investigations to evaluate the results and to find the best management practices for the given location and problem.

This study will be expanded to categorize PSI data indicating subsidence by trends in timeseries and combining them with other datasets. This would increase the knowledge of the subsurface processes and the effects of interventions, and thereby ultimately identify effective actions to decrease effects related to the urban water cycle.

Further, end-users should be involved in the development of risk assessment maps, for example in the evaluation of the usability of prototypes, like the ones presented here. Choosing an adequate method for risk assessment with the end-user tasks in focus is important and will give more applicable results. Trying out multiple methods for analysis and visual analysis for quality control of map results was emphasized in this study and is strongly recommended in further studies.

ACKNOWLEDGEMENTS

This research is supported through the Water JPI funded the INXCES research project 'INnovation for eXtreme Climatic EventS' www.inxces.eu. Sentinel-1A/B images are provided by the European Space Agency (ESA). Thanks to the Norwegian Ground Motion Services for open and accessible data, www.insar.no. We greatly appreciate the help of John Dehls (NGU). We thank the Bergen Municipality, Tauw and Hogeschool van Amsterdam, the Hanze University of Applied Sciences, Groningen, for support for this work. Thanks to the Norwegian Hydrology Council for the NHC2018 conference in Bergen and this special conference issue. Great appreciation for the support of Anne Liinamaa-Dehls at the Geological Survey of Norway (NGU) during proof-reading and editing of this article. Great appreciation to two anonymous reviewers and the special issue editor of *Journal of Hydrology Research*, Kolbjørn Egeland, for improving this paper.

REFERENCES

Albano, R., Mancusi, L. & Abbate, A. 2017 Improving flood risk analysis for effectively supporting the implementation of flood risk management plans: the case study of 'Serio' valley. *Environmental Science & Policy* **75**, 158–172.

Albano, R., Sole, A., Adamowski, J., Perrone, A. & Inam, A. 2018 Using FloodRisk GIS freeware for uncertainty analysis of direct economic flood damages in Italy. *International Journal of Applied Earth Observation and Geoinformation* **73**, 220–229. https://doi.org/10.1016/j.jag.2018.06.019.

Balstrøm, T. & Crawford, D. 2018 Arc-Malstrøm: A 1D hydrologic screening method for stormwater assessments based on geometric networks. *Computers and Geosciences* **116**, 64–73. https://doi.org/10.1016/j.cageo.2018.04.010.

Berardino, P., Costantini, M., Franceschetti, G., Iodice, A., Pietranera, L. & Rizzo, V. 2003 Use of differential SAR interferometry in monitoring and modelling large slope instability at Maratea (Basilicata, Italy). *Engineering Geology* **68**, 31–51. doi:10.1016/S0013-7952(02)00197-7.

Bergen kommune 2006 Hovedplan for avløp og vannmiljø 2005-2015. Bystyrets Kontor (ed.). Bergen, Norge: Bergen kommune (In Norwegian).

Bolund, P. & Hunhammar, S. 1999 Ecosystem services in urban areas. *Ecological Economics* **29**, 293–301.

Boogaard, F. C. 2015 Stormwater quality and sustainable urban drainage management. In: *Monitoring, Mitigation, Management: The Groundwater Project – Safeguarding the World Heritage Site of Bryggen in Bergen* (J. Rytter & I. Schonhowd, eds). Riksantikvaren, Bergen, pp. 136–149.

Boogaard, F. C., Wentink, R., Vorenhout, M. & de Beer, J. 2016 Implementation of sustainable urban drainage systems to preserve cultural heritage – pilot Motte Montferland. *Journal of Conservation and Management of Archaeological Sites* **18** (1–2), 328–341. https://doi.org/10.1080/13505033.2016.1182767.

Boogaard, F. C., Vojinovic, Z., Chen, Y.-C., Kluck, J. & Lin, T.-P. 2017a High Resolution Decision Maps for Urban Planning: A Combined Analysis of Urban Flooding and Thermal Stress Potential in Asia and Europe. In *MATEC Web of Conferences*. 103, 04012. ISCEE 2016. doi:10.1051/matecconf/201710304012.

Boogaard, F. C., Kluck, J., Bosscher, M. & Schoof, G. 2017b Flood model Bergen Norway and the need for (sub-)surface INnovations for eXtreme Climatic EventS (INXCES). *Procedia Engineering* **209**, 56–60. doi:10.1016/j.proeng.2017.11.130.

Boogaard, F. C., Krol, D., Kluck, J. & Bosscher, M. 2018 Multi-Level Climate Effect Modeling, best management practices From private property to national level, Cirre 2018. In: *Conference of Interdisciplinary Research on Real Estate*, September 2018, Groningen.

Campbell, D., de Beer, J., Mielby, S., van Campenhout, I., van der Meulen, M., Erikkson, I., Venvik Ganerod, G., Lawrence, D., Bacic, M., Donald, A., Gogu, C. R. & Jelenek, J. 2017 Transforming the relationship between geoscientists and urban decision-makers. European COST Sub-Urban Action (TU1206). *Procedia Engineering* **209**, 4–11. doi:10.1016/j.proeng.2017.11.124.

Carver, S. J. 1991 Integrating multi-criteria evaluation with geographical information systems. *International Journal of Geographical Information Systems* **5** (3), 321–339.

Castellazzi, P., Arroyo-Domínguez, N., Martel, R., Calderhead, A. I., Normand, J. C. L., Gárfias, J. & Rivera, A. 2016 Land subsidence in major cities of Central Mexico: interpreting InSAR-derived land subsidence mapping with hydrological data. *International Journal of Applied Earth Observation and Geoinformation* **47**, 102–111. http://dx.doi.org/10.1016/jag2015.12.002.

Chaussard, E., Wdowinski, S., Cabral-Cano, E. & Amelung, F. 2014 Land subsidence in central Mexico detected by ALOS InSAR time-series. *Remote Sensing of Environment* **140**, 94–106. https://doi.org/10.1016/j.rse.2013.08.038.

Crosetto, M., Monserrat, O., Cuevas-González, M., Devanthéry, N. & Crippa, B. 2016 Persistent Scatterer Interferometry: A review. *Journal of Photogrammetry and Remote Sensing* **115**, May 2016, 78–89.

Damoom, M. M., Hashim, S., Aljohani, M. S., Saleh, M. A. & Xoubi, N. 2019 Potential areas for nuclear power plant siting in Saudi Arabia: GIS-based multi-criteria decision making analysis. *Progress in Nuclear Energy* **110**, 110–120. https://doi.org/10.1016/j.pnucene.2018.09.018.

de Beer, J. D. & Seither, A. 2015 Groundwater balance. In: *Monitoring, Mitigation, Management: The Groundwater*

Project – Safeguarding the World Heritage Site of Bryggen in Bergen (J. Rytter & I. Schonhowd, eds). Riksantikvaren, Bergen, Norway, pp. 106–123.

de Beer, J. D., Matthiesen, H. & Christensson, A. 2012 Quantification and visualization of in situ degradation at the World Heritage Site Bryggen in Bergen, Norway. *Conservation and Management of Archaeological Sites* **14**, 215–227.

Directorate for Cultural Heritage (Riksantikvaren) 2018 Cultural layers vector data. https://www.riksantikvaren.no/.

Dixon, T. H., Amelung, F., Ferretti, A., Novali, F., Rocca, F., Dokka, R., Sella, G., Kim, S.-W., Widowinski, S. & Whitman, D. 2006 Subsidence and flooding in New Orleans. *Nature* **441** (7093), 587–588. https://doi.org/10.1038/441587a.

Erbaş, M., Kabak, M., Özceylan, E. & Çetinkaya, C. 2018 Optimal siting of electric vehicle charging stations: a GIS-based fuzzy Multi-Criteria Decision Analysis. *Energy* **163**, 1017–1031. https://doi.org/10.1016/j.energy.2018.08.140.

Eriksen, H. Ø., Lauknes, T. R., Larsen, Y., Corner, G. D., Bergh, S. G., Dehls, J. & Kierulf, H. P. 2017 Visualizing and interpreting surface displacement patterns on unstable slopes using multi-geometry satellite SAR interferometry (2D InSAR). *Remote Sensing of Environment* **191**, 297–312. https://doi.org/10.1016/j.rse.2016.12.024.

Ersland, G. A. 2015 The history of Bryggen until C. 1900. In: *Monitoring, Mitigation, Management: The Groundwater Project – Safeguarding the World Heritage Site of Bryggen in Bergen* (J. Rytter & I. Schonhowd, eds). Riksantikvaren, Bergen, pp. 12–23.

ESRI 2018 *ArcPro 2.3.1*. Environmental System Research Institute, Redlands, CA.

ESRI 2019 http://desktop.arcgis.com/en/arcmap/10.3/tools/spatial-statistics-toolbox/hot-spot-analysis.htm

Fletcher, T. D., Andrieu, H. & Hamel, P. 2013 Understanding, management and modelling of urban hydrology and its consequences for receiving waters: a state of the art. *Advances in Water Resources* **51**, 261–279. https://doi.org/10.1016/j.advwatres.2012.09.001.

Getis, A. & Ord, J. K. 1992 The analysis of spatial association by use of distance statistics. *Geographical Analysis* **24** (3), 189–206. doi:10.1111/j.1538-4632.1992.tb00261.x.

Google Earth 2019 Bergen City 60°24'11"N, 5°19'23"W, 3D map, viewed 30 April 2019. https://earth.google.com/web/.

Hansen, G. 1994 Den overordnede bebyggelsestopografi omkring 1190 i Bergen: belyst ut fra arkæologiske, naturtopografiske og skriftlige kilder. Riksantikvaren, Utgravningskontoret for Bergen (In Norwegian).

Hanssen, G. S. 2018 Planlegging for risikosamfunnet: Hvordan fungerer flomsonekart med klimapåslag som kunnskapsoversettelse? Kart og Plan 1-2018, pp. 17-36 (In Norwegian).

Hanssen-Bauer, I., Førland, E. J., Haddeland, I., Hisdal, H., Lawrence, D., Mayer, S., Nesje, A., Nilsen, J. E. Ø., Sandven, S., Sandø, A. B., Sorteberg, A. & Ådlandsvik, B. 2017 *Climate in Norway 2100 – A Knowledge Base for Climate Adaptation*. NCCS Report no. 1/2017. M-741/2017. ISSN nr. 2387-3027.

Harvold, K., Larsen, K., de Beer, J., Boogaard, F., Vandrup Martens, V., Matthiesen, H., Muthanna, T. M., Seither, A., Skogheim, R. & Vorenhout, M. 2015 (Urban WATCH), ISBN: 978-82-92935-13-2, CIENS Report 2015:1

Haughton, G. & Hunter, C. 1994 *Sustainable Cities*. UK Jessica Kingsley Publishers, London, pp. 357.

Haukedal, J. 2017 *Setningsutvikling i Bergen sentrum: Urbanhydrogeologi, InSAR, setning og kulturlag*. Master Thesis, Natural Geography at the University of Bergen. (In Norwegian).

Hooimeijer, F. L., Lafleura, F. & Trinh, T. T. 2017 Drawing the subsurface: an integrative design approach. *Procedia Engineering* **209**, 61–74. doi:10.1016/j.proeng.2017.11.131.

IPCC 2014 Climate change 2014: impacts, adaptation, and vulnerability. Part A: Global and sectoral aspects. In: *Contribution of Working Group II to the Fifth Assessment Report of the Intergovernmental Panel on Climate Change* (C. B. Field, V. R. Barros, D. J. Dokken, K. J. Mach, M. D. Mastrandrea, T. E. Bilir, M. Chatterjee, K. L. Ebi, Y. O. Estrada, R. C. Genova, B. Girma, E. S. Kissel, A. N. Levy, S. MacCracken, P. R. Mastrandrea & L. L. White, eds). Cambridge University Press, Cambridge, UK and New York, NY, USA, pp. 1–1132.

Jensen, J. A. 2004 *Vurdering og tolkninger av setningsmålinger*. Report No. 400425-6. Multiconsult avd. NOTEBY (In Norwegian).

Jensen, J. A. 2015 Subsidence at the Bryggen site. In: *Monitoring, Mitigation, Management: The Groundwater Project – Safeguarding the World Heritage Site of Bryggen in Bergen* (J. Rytter & I. Schonhowd, eds). Riksantikvaren, Bergen, pp. 152–164.

Kluck, J., Claessen, E. G., Blok, G. M. & Boogaard, F. C. 2010 Modelling and mapping of urban storm water flooding, communication and prioritizing actions through mapping urban flood resilience. *NOVATECH 2010*.

Kluck, J., Boogaard, F. C., Goedbloed, D. & Claassen, M. 2015 Storm Water Flooding Amsterdam, from a quick Scan analyses to an action plan. In *International Waterweek 2015*, 3 November 2015, Amsterdam.

Lauknes, T. R., Piyush Shanker, A., Dehls, J. F., Zebker, H. A., Henderson, I. H. C. & Larsen, Y. 2010 Detailed rockslide mapping in northern Norway with small baseline and persistent scatterer interferometric SAR time series methods. *Remote Sensing of Environment* **114**, 2097–2109. https://doi.org/10.1016/j.rse.2010.04.015.

Lu, P., Casagli, N., Catani, F. & Tofani, V. 2012 Persistent Scatterers Interferometry Hotspot and Cluster Analysis (PSI-HCA) for detection of extremely slow-moving landslides. *International Journal of Remote Sensing* **33** (2), 466–489. doi:10.1080/01431161.2010.536185.

Lyu, H. M., Sun, W. J., Shen, S. L. & Arulrajah, A. 2018 Flood risk assessment in metro systems of mega-cities using a GIS-based modelling approach. *Science of the Total Environment* **626**, 1012–1025. https://doi.org/10.1016/j.scitotenv.2018.01.138.

Mangerud, J. 2004 Ice sheet limits in Norway and on the Norwegian continental shelf. In: *Quaternary Glaciations – Extent and Chronology: Europe*, Vol. 1 (J. Ehlers & P. Gibbard, eds). Elsevier, Amsterdam, pp. 271–294.

Marsalek, J. & Chocat, B. 2002 International report: stormwater management. *Water Science & Technology* **46** (6–7), 1–17. https://doi.org/10.2166/wst.2002.0657.

Marsalek, J., Jiménez-Cisneros, B. E., Malmquist, P.-A., Karamouz, M., Goldenfum, J. & Chocat, B. 2006 *Urban Water Cycle Process and Interactions*. UNESCO Publishing and Taylor and Francis Group, Paris.

Matthiesen, H., Hollesen, J. & Gregory, D. 2015 Preservation Conditions and Decay Rates. In: *Monitoring, Mitigation, Management: The Groundwater Project – Safeguarding the World Heritage Site of Bryggen in Bergen* (J. Rytter & I. Schonhowd, eds). Riksantikvaren, Bergen, pp. 76–91.

Mignot, E., Li, X. & Dewals, B. 2019 Experimental modelling on urban flooding: a review. *Journal of Hydrology* **568**, 334–342. https://doi.org/10.1016/j.jhydrol.2018.11.001.

Miller, J. & Hutchins, M. 2017 The impacts of urbanisation and climate change on urban flooding and urban water quality: a review of the evidence concerning the United Kingdom. *Journal of Hydrology: Regional Studies* **12**, 345–362. http://dx.doi.org/10.1016/j.ejrh.2017.06.006.

Miller, R. L., Fram, M. S., Fujii, R. & Wheeler, G. 2008 Subsidence reversal in a re-established wetland in the Sacramento-San Joaquin Delta, California, USA. *San Francisco Estuary and Watershed Science* **6** (3). article 1.

Motagh, M., Shamshiri, R., Haghighi, M. H., Wetzel, H.-U., Akbari, B., Nahavandchi, H., Roessner, S. & Arabi, S. 2017 Quantifying groundwater exploration induced subsidence in the Rafsanjan plain, southeastern Iran, using InSAR time-series and in situ measurements. *Journal of Engineering Geology* **2018**, 134–151. http://dx.doi.org/10.1016/j.enggeo.2017.01.011.

Norwegian Directorate for Civil Protection (DSB) 2017 Integrating Sea Level Rise and Storm Surges in Local Planning. ISBN 978-82-7768-447-5 (PDF). Available from: https://www.dsb.no/globalassets/dokumenter/veiledere-handboker-og-informasjonsmateriell/veiledere/integrating-sea-level-rise-and-storm-surges-in-local-planning.pdf

Norwegian Ground Motion Center 2018 Interferometric synthetic-aperture radar data 2016-2018. Available from: http://www.insar.no

Norwegian Map Authority (Kartverket) 2009 Produktspesifikasjon FKB-Laser Versjon 2.0 2009-02-01, Produktspesifikasjon Nasjonal modell for høydedata fra laserskanning (FKB-Laser), *Statens kartverk* 2009.

Norwegian Map Authority (Kartverket) 2018 Topographical data, sea level and storm surges. Available from: https://www.kartverket.no/sehavniva/.

Norwegian Meteorological Institute (NMI) 2019 Available from: https://www.yr.no/place/Norway/Hordaland/Bergen/Bergen/statistics.html.

Pregnolato, M., Ford, A., Glenis, V., Wilkinson, S. & Dawson, R. 2017 Impact of climate change on disruption to urban transport networks from pluvial flooding. *Journal of Infrastructure Systems* **23** (4). doi:10.1061/(ASCE)IS.1943-555X.0000372.

Rytter, J. & Schonhowd, I. (eds) 2015a *Monitoring, Mitigation, Management: The Groundwater Project – Safeguarding the World Heritage Site of Bryggen in Bergen*. Riksantikvaren, Bergen, pp. 213. ISBN: 978-82-7574-085-2. Available from: http://prosjektbryggen.no/publikasjoner/.

Rytter, J. & Schonhowd, I. 2015b Operation groundwater rescue. In: *Monitoring, Mitigation, Management: The Groundwater Project – Safeguarding the World Heritage Site of Bryggen in Bergen* (J. Rytter & I. Schonhowd, eds). Riksantikvaren, Bergen, pp. 50–59.

Schmidt, D. A. & Bürgmann, R. 2003 Time-dependent land uplift and subsidence in the Santa Clara valley, California, from a large interferometric synthetic aperture radar data set. *Journal of Geophysical Research September 2003*. https://doi.org/10.1029/2002JB002267.

Sörensen, J. & Mobini, S. 2017 Pluvial, urban flood mechanisms and characteristics – assessment based on insurance claims. *Journal of Hydrology* **555**, 51–67. https://doi.org/10.1016/j.jhydrol.2017.09.039.

Statistics Norway (SSB) 2017 Available from: https://www.ssb.no/befolkning/statistikker/folkemengde/aar-per-1-januar/#relatert-tabell-1.

Teatini, P., Tosi, L., Strozzi, T., Carbognin, L., Cecconi, G., Rosselli, R. & Libardo, S. 2012 Resolving land subsidence within the Venice Lagoon by persistent scatterer SAR interferometry, Physics and Chemistry of the Earth, Parts A/B/C, **40–41**, 72–79. ISSN 1474-7065.

Thornbush, M., Golubchikov, O., Golubchikov, O. & Bouzarovski, S. 2013 Sustainable cities targeted by combined mitigation-adaptation efforts for future-proofing. *Sustainable Cities and Society* **9**, 1–9. http://dx.doi.org/10.1016/j.scs.2013.01.003.

United Nations, Department of Economic and Social Affairs, Population Division 2016 The World's Cities in 2016 - Data Booklet (ST/ESA/ SER.A/392). Available from: https://www.un.org/en/development/desa/population/publications/pdf/urbanization/the_worlds_cities_in_2016_data_booklet.pdf

UN-Water 2018 *United Nations World Water Assessment Programme, 2018*. The United Nations World Water Development Report 2018: Nature-Based Solutions for Water. UNESCO, Paris. Available from: http://www.unesco.org/new/en/natural-sciences/environment/water/wwap/wwdr/2018-nature-based-solutions/.

Wakode, H. B., Baier, K., Jha, R. & Azzam, R. 2018 Impact of urbanization on groundwater recharge and urban water balance for the city of Hyderabad, India. *International Soil and Water Conservation Research* **6**, 51–62. https://doi.org/10.1016/j.iswcr.2017.10.003.

Yin, J., Yu, D. & Wilby, R. 2016 Modelling the impact of land subsidence on urban pluvial flooding: a case study of downtown Shanghai, China. *Science of the Total Environment* **544**, 744–753. http://dx.doi.org/10.1016/j.scitotenv.2015.11.159.

First received 1 March 2019; accepted in revised form 2 December 2019. Available online 31 December 2019